

# Design and Implementation of a Two-Cell Sample Holder for High Field Electron Paramagnetic Resonance Spectrometers

Angie Yao<sup>1†</sup>, Antonín Sojka<sup>2</sup>

<sup>1</sup>Northgate High School, 425 Castle Rock Rd, Walnut Creek, CA 94598

<sup>2</sup>Department of Physics, University of California, Santa Barbara, CA 93106

<sup>3</sup>Institute for Terahertz Science and Technology

<sup>†</sup>Corresponding author: angie.fyao@gmail.com

Sherwin Group

Driven Quantum and Biological Matter

UC SANTA BARBARA

Research Mentorship Program



## Abstract

- Quasi-optical sample holders for Electron Paramagnetic Resonance (EPR) spectrometers currently measure **one sample**
- Coupling between sample and microwave varies with each sample exchange and decreases efficiency of measurements
- We design, 3D print, and troubleshoot two-cell SH to exchange samples inside the probe
- Our sample holder integrated into spectrometer under temperatures of 1.6-300 K, frequency of 240 GHz, and magnetic fields up to 12 T
- Quantitative measurements** made comparing two liquid TEMPO samples

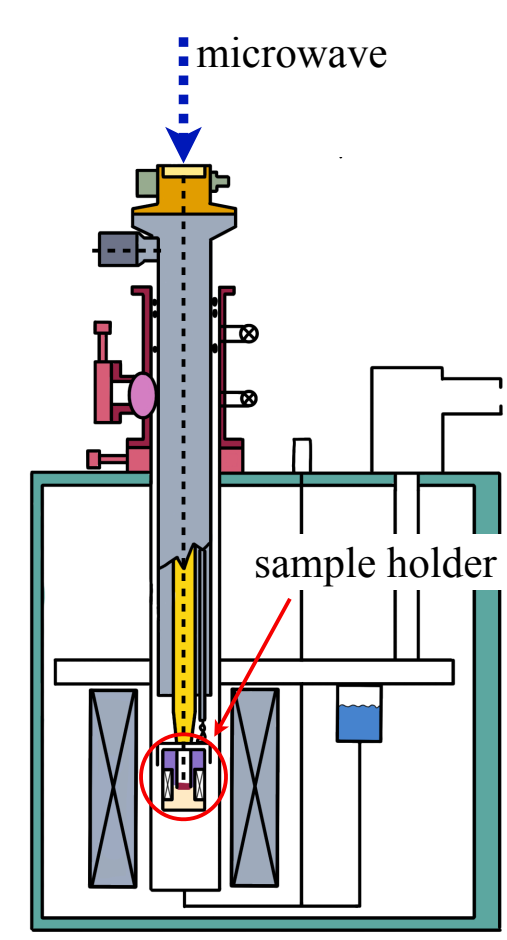


FIG. 1. Diagram of EPR probe inside the superconducting cryogen-free magnet (adapted from [4])

## EPR Spectroscopy

### Zeeman Effect

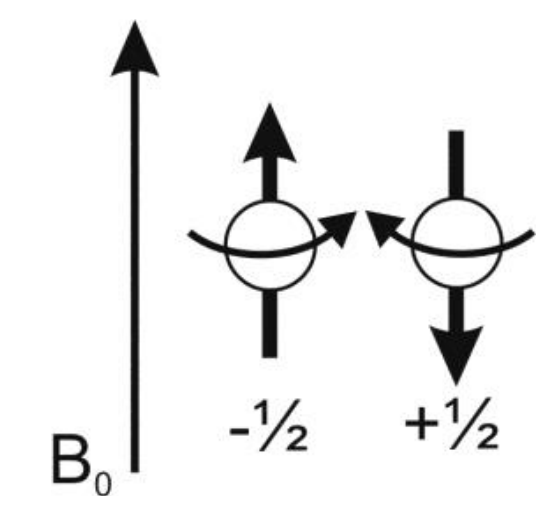


FIG. 2. Alignment of electron's magnetic moment to the field [1]

- Energy differences** created by interaction between unpaired electron spins in external magnetic field
- For single unpaired electron spin ( $S = 1/2$ ),  $m_s = -1/2$  or  $m_s = +1/2$
- lowest energy when aligned parallel ( $m_s = -1/2$ )
- highest energy when aligned antiparallel ( $m_s = +1/2$ ) [1]

### g-Factor

- Characterizes **magnetic moment** and **angular momentum** of structures with unpaired electrons
- Remains constant regardless of microwave frequency, making it a **reliable fingerprint** for each measured system
- To calculate  $g$ -factor for quantitative EPR, the resonance condition is used as given by equation 1 [2]:

$$\Delta E = E_1 - E_2 = hf = g\mu_B B_{Res} \quad (1)$$

### Derivative Spectra

- Modulation coil generates oscillating magnetic field,  $B_{mod}$ , at a few kHz to improve Signal-to-Noise-Ratio (SNR)
- Converts weak signal into easily detectable modulated signal
- At  $B_0 = 0$ , the energy difference between spin states is degenerate
- At  $B_0 \neq 0$ , two energy states  $E_1$  and  $E_2$  are separated by  $\Delta E$
- At  $hf = \Delta E$ , absorption signal detected [3]
- $B_{mod}$  modulates the x-axis which results in the **first derivative** of the absorption EPR signal [4]

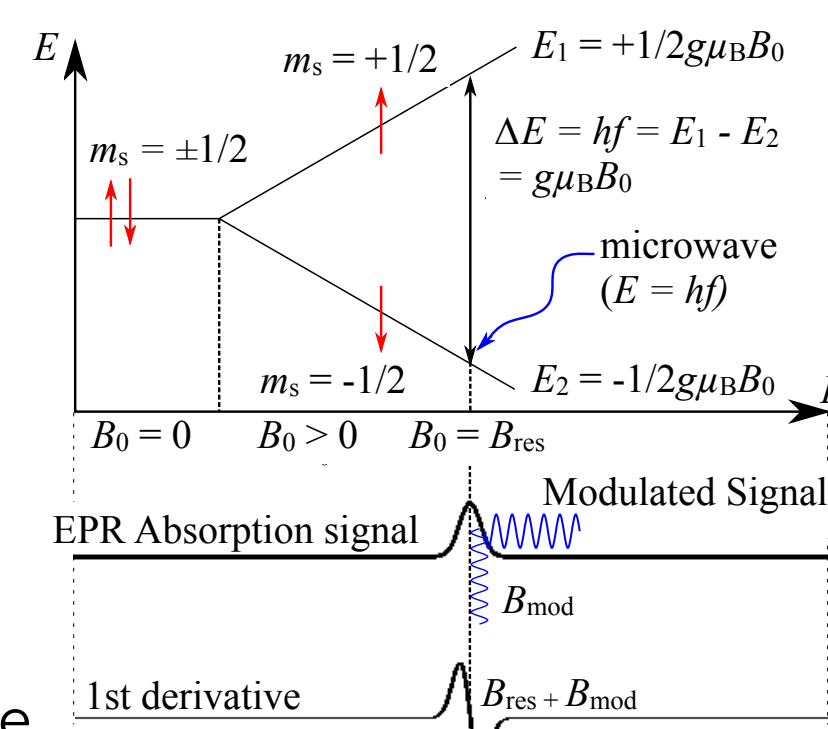


FIG. 3. Diagram showing the interaction between an electron spin ( $S = 1/2$ ) with an external magnetic field,  $B_0$ , and the frequency ( $f$ ) of an oscillating electromagnetic irradiation. When the microwave radiation matches the gap at the absorption signal, the lower energy levels flip to a higher energy level [4]

## High-Frequency EPR

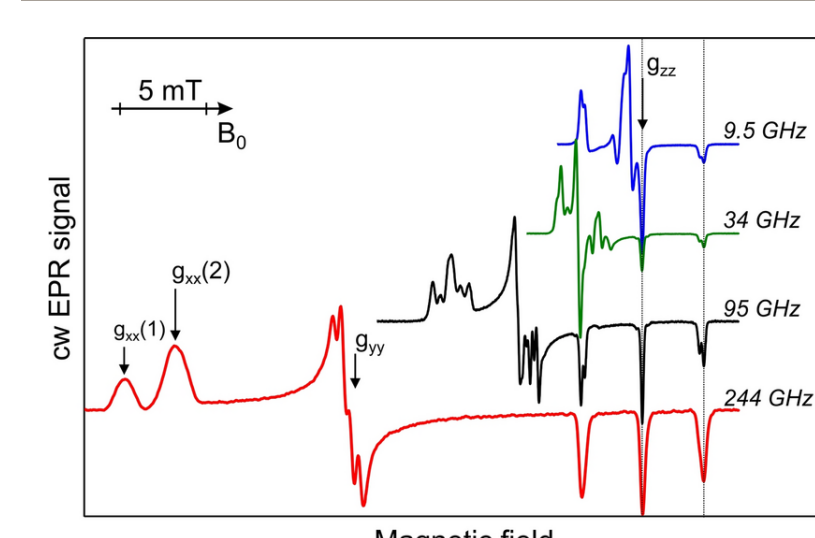


FIG. 4. Enhanced signal detection via HF-EPR [5]

- High-Frequency EPR (HF-EPR) increases **spectrometer resolution** and **sensitivity** to enable the study of high spin systems [5]
- Operates at high frequencies above 100 GHz and magnetic fields above 3.5 T [6]

## Quasi-Optical Sample Holder

- Focusing quasi-optics keep microwave beam within specified path
- Enhanced field modulation amplitude and homogeneity on the sample
- Rooftop and parabolic mirror **improve SNR by 6** to detect signal
- Functions in continuous-wave, pulsed, and rapid-scan EPR modes [7]
- 3D printed with exception of rooftop mirror, parabolic mirror, and coil
- Limitations due to ability to only measure **one sample** at a time

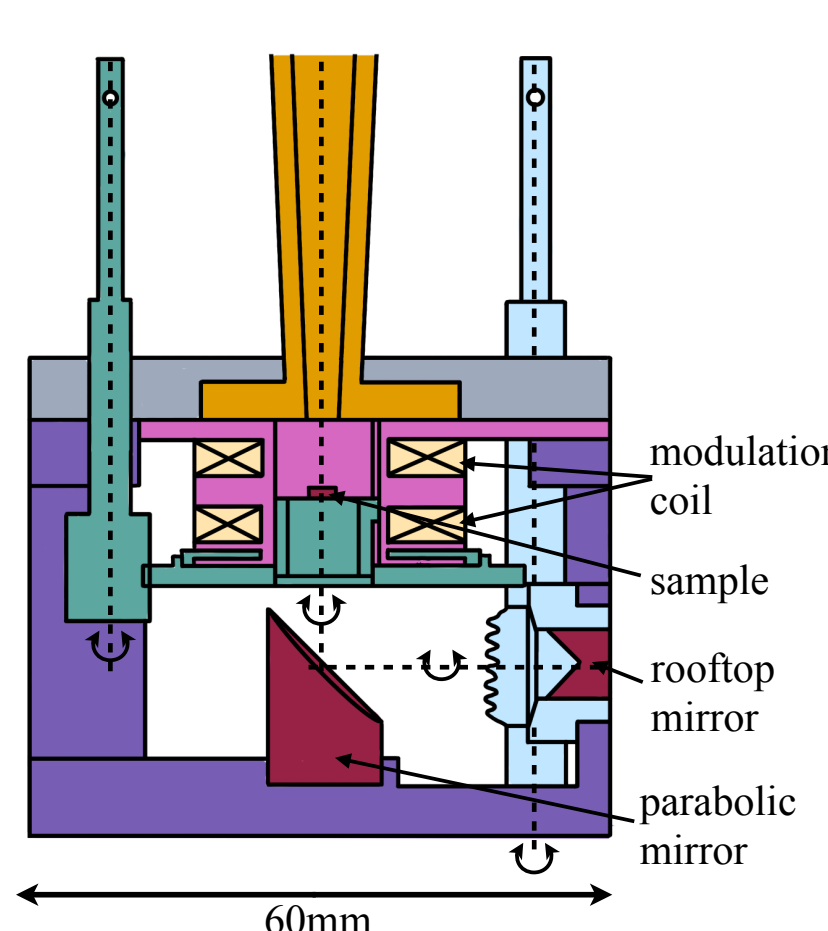


FIG. 5. Diagram of the quasi-optical sample holder (adapted from [7])

## Research Objectives

- Design a sample holder that can switch between two samples within the probe in Onshape
- 3D print and troubleshoot using fused deposition modeling printer
- Implement 3D printed two-cell sample holder into HF-EPR
- Make **quantitative comparisons** between two liquid TEMPO samples with different concentrations

## Two-Cell Sample Holder

- Two spaces 5 mm in diameter for each sample
- Attached to end of 1 m long probe (microwave waveguide)
- Mechanical feedthrough to switch samples
- Sample located 9 mm under a corrugated waveguide
- Magnet bore diameter of 60 mm
- Mirror with diameter of 7.01 mm and height of 2.13 mm placed 2.478 mm under the sample
- Distance between sample and mirror must be a multiple of the **wavelength number** (1.239 mm for 240 GHz)
- Ensures that sample sits on maximum oscillating magnetic component of microwave radiation [8]

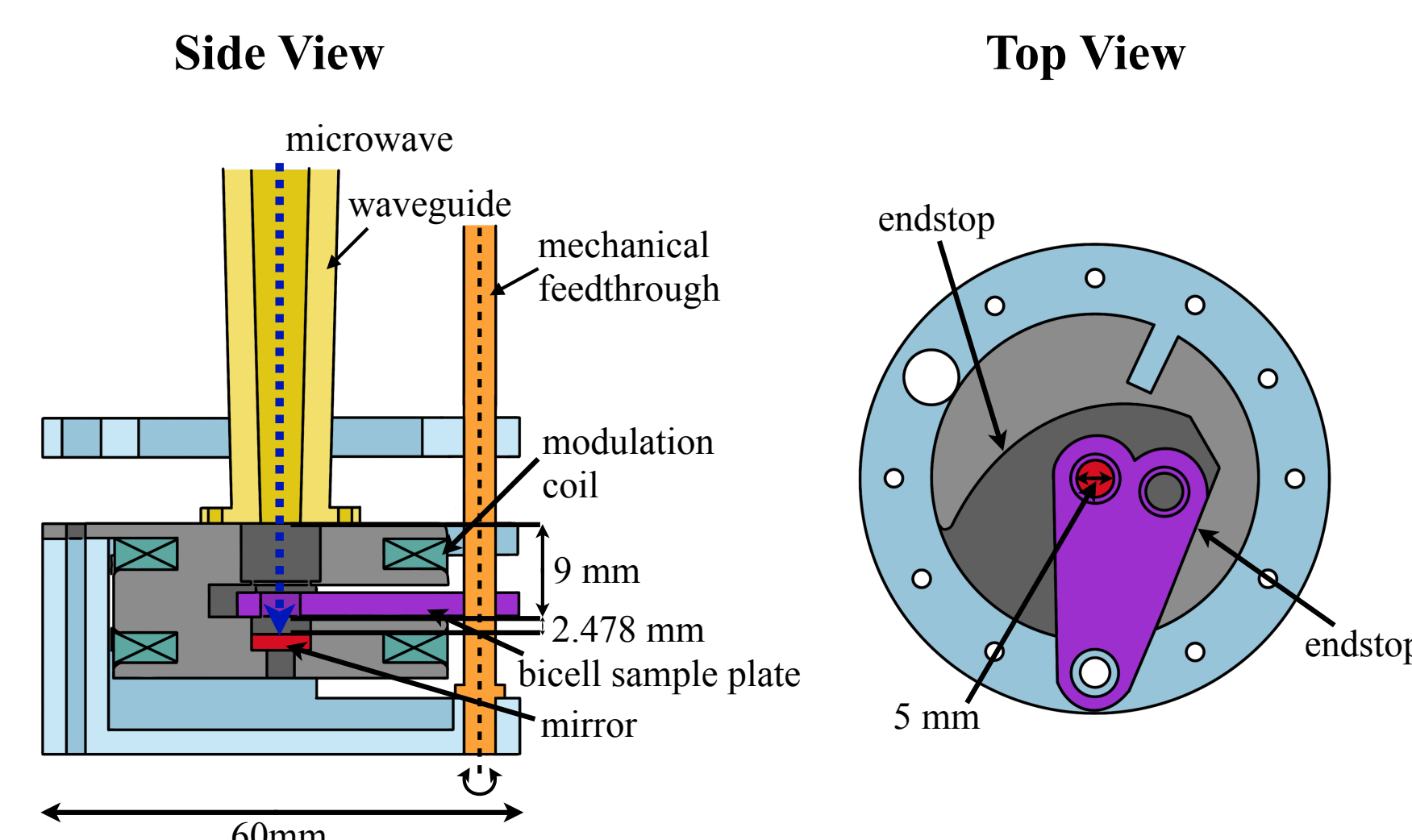


FIG. 6. Proposed design for the 3D printed two-cell sample holder and modulation coil

## Calibration using LiPc Crystal

- Modulation coil calibrated using lithium phthalocyanine (LiPc) crystal
- Coil wound from Cu32 American Wire Gauge using 200 revolutions
- Measured at 40 mW and 240 GHz
- Amplitude normalized by dividing measurements by largest value
- Measured  $g$ -factor was **2.005** compared to actual 2.0024 [9]
- Typical error is 18 G due to variation in main field
- Modulation coil operated at **0.3 G/mA**

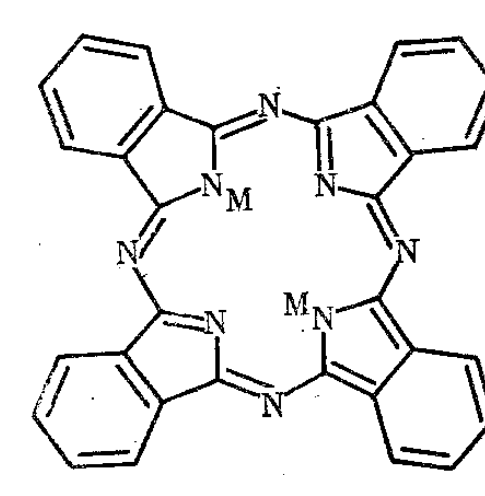


FIG. 7. LiPc crystal [9]

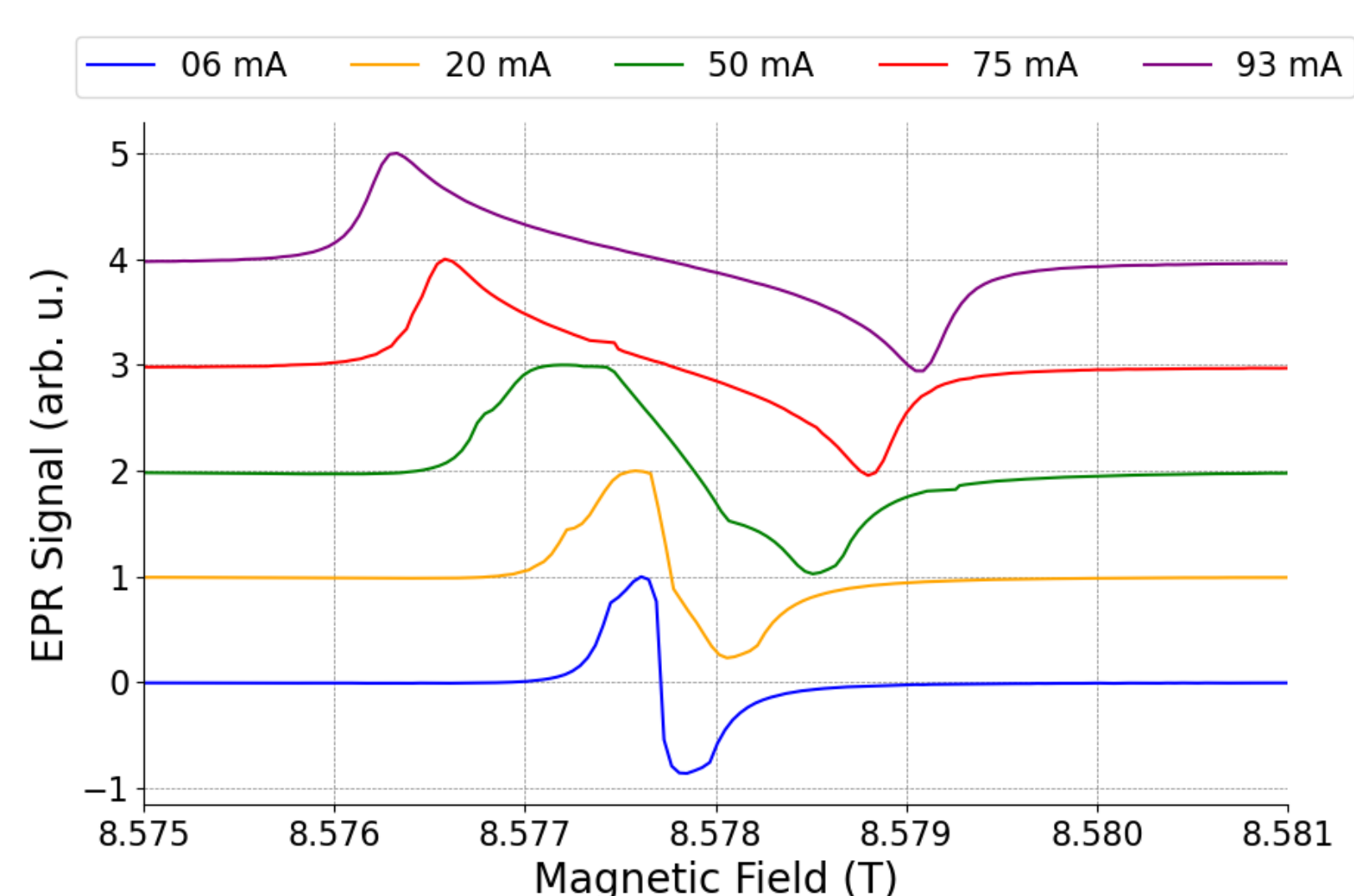


FIG. 8. The difference in linewidths of the LiPc crystal at five currents: 6, 20, 50, 75, and 93 mA

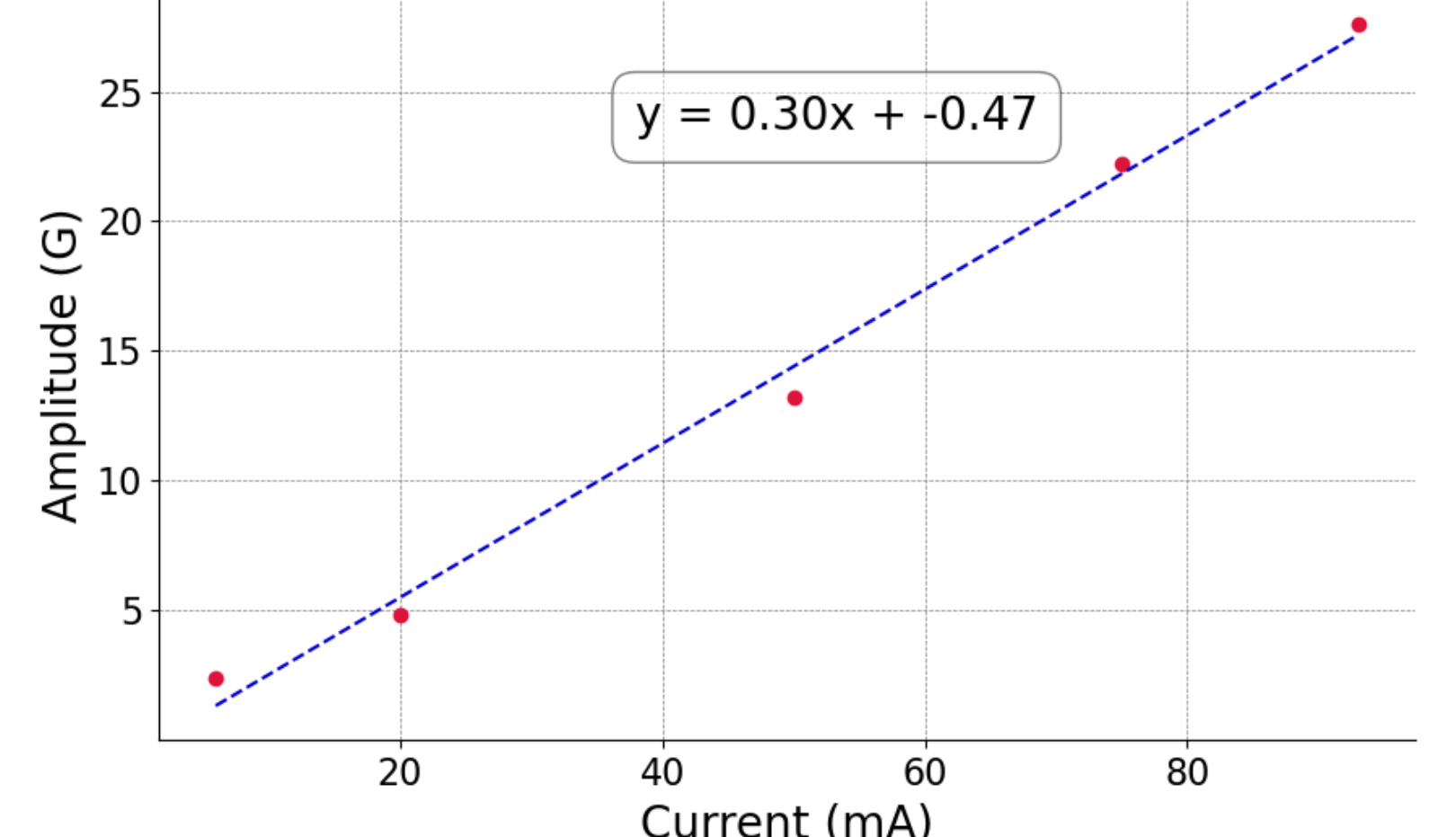


FIG. 9. The modulation coil amplitude as a function of the current. The dashed line represents the linear fit

## Liquid TEMPO Samples

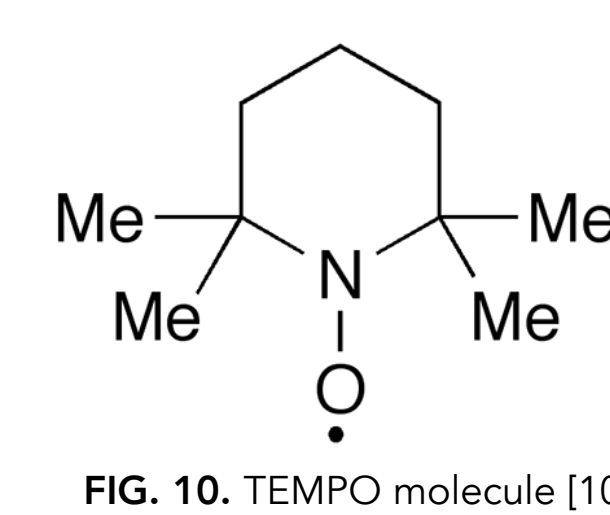


FIG. 10. TEMPO molecule [10]

- First sample is 10 mg TEMPO dissolved in 1 mL toluene, **2.5 mM**
- Second sample is 10 mg TEMPO dissolved in 10 mL toluene, **0.25 mM**
- 1.6  $\mu$ L of each solution inserted into 3 mm long flat cell

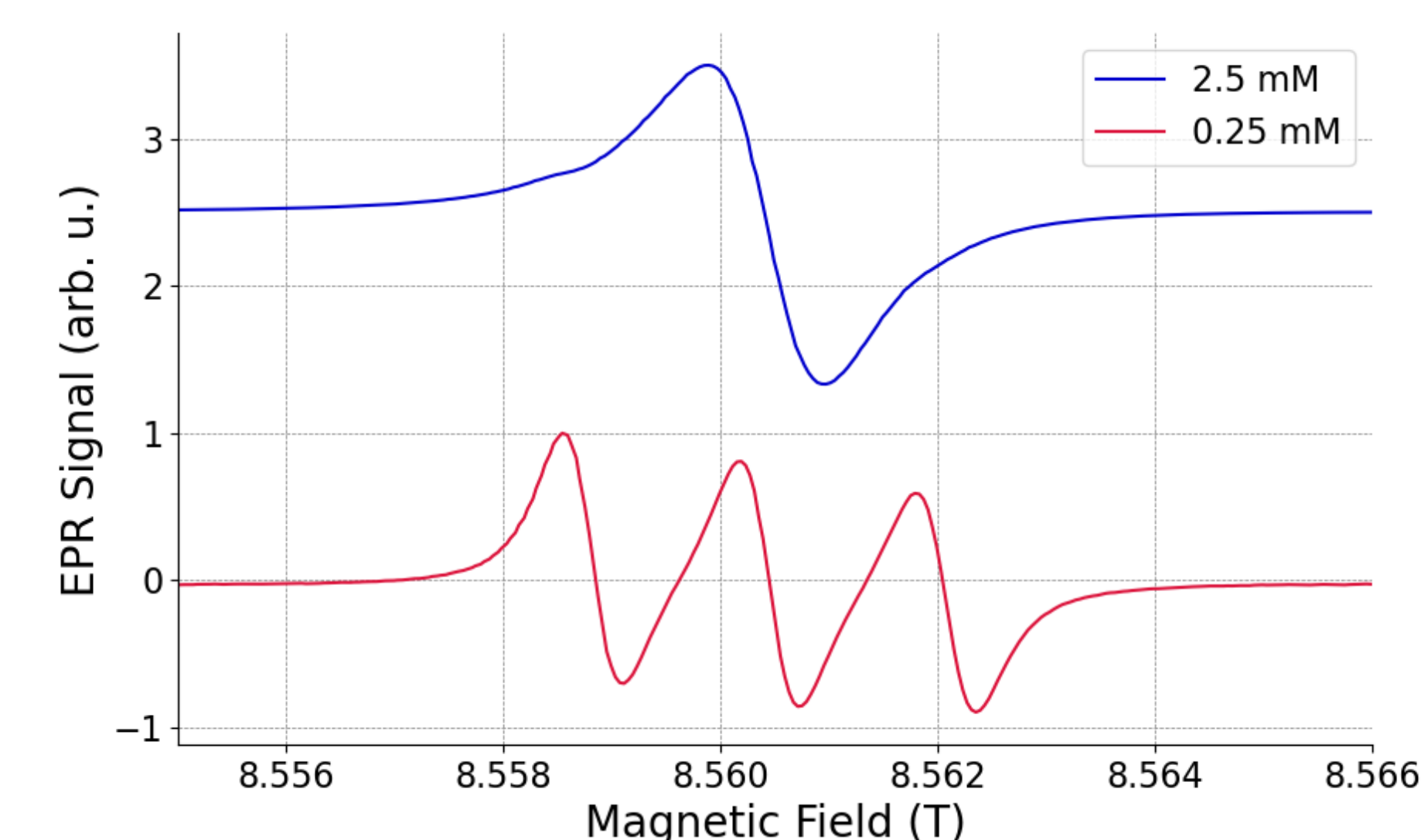


FIG. 11. EPR signal of 2.5 mM and 0.25 mM of TEMPO dissolved in toluene

- Hyperfine interactions cause **three peaks** for 0.25 mM sample
- Linewidth of 2.5 mM sample broader due to **spin-spin relaxation** time and **hyperfine interactions**
- Average distance ( $r$ ) between two spins from the concentration ( $n$ ) calculated using equation 2 [11]:

$$\langle r \rangle = \int_0^\infty r w(r) dr = \Gamma(4/3)/(4\pi/3)^{1/3} = 0.55396n^{-1/3} \quad (2)$$

	Linewidth	Spin-spin distance	Signal-to-Noise-Ratio
2.5 mM	1.1 mT	4 nm	2500
0.25 mM	0.549 mT	10 nm	430

TABLE 1. The observed linewidth, spin-spin distance, and SNR for the 2.5 mM and 0.25 mM samples

- Difference in SNR is **6** times compared to expected 10 times because concentration is 10 times smaller, errors may result mostly from line shape but also from concentration and position variations
- Resonance condition changes due to splitting of energy levels
- Spin states split by exchange interaction, which alters position of EPR signal
- When  $S_1 = S_2 = 1/2$ , energy levels split into singlet ( $S = 0$ ) and triplet ( $S = 1$ ) states
- At low concentration (0.25 mM), TEMPO molecules spaced far apart
  - Hyperfine interactions occur between **unpaired electron** and **nitrogen nucleus** ( $S = 1$ )
  - Nucleus has three spin states (-1, 0, +1)
  - Splits EPR signal into three peaks [12]
- At high concentration (2.5 mM), TEMPO molecules are spaced closer together
  - Electron-electron interactions** occur
  - Electron has two spin states (-1/2, +1/2)
  - Three hyperfine peaks average out and broaden into **single peak**, called exchange narrowing [13]

## Findings and Impact



FIG. 12. Two-cell sample holder printed from polylactic acid using the Original Prusa i3 MK3S+ 3D printer

- Three peaks observed for 0.25 mM TEMPO compared to 2.5 mM TEMPO due to Heisenberg interaction
- Reduced downtime between measurements by **five hours**
- Improved SNR for higher accuracy measurements
- Enables quantitative measurements

## Future Work

- Incorporate the two-cell sample holder into the quasi-optical sample holder
- Conduct quantitative AsLOV2 protein measurements
- Enable sample loading within the probe

## Acknowledgements:

We would like to thank Dr. Mark Sherwin, Dr. Lina Kim, Brad Price, Alex Giovannone, Johanna Schubert, Miranda Claypool, Leonardo Ramirez-Mireles, Casey Bernd, Wei-Hsu Lin, Leila Elrgdaw, all the members of the Sherwin Group, and Pratyush Tripathy for their feedback, guidance, and support throughout this entire project.

## References:

- [1] L. Arda, "The effects of Tb doped ZnO nanorod: An EPR study," *Journal of Magnetism and Magnetic Materials*, vol. 475, pp. 493–501, Apr. 2019, doi: <https://doi.org/10.1016/j.jmmm.2018.11.121>.
- [2] J. L. Stahlik, "An electron spin resonance magnetometer for time-varying fields," *Nuclear Instruments and Methods*, vol. 17, no. 2, pp. 157–160, Oct. 1962, doi: [https://doi.org/10.1016/0029-554x\(62\)90155-6](https://doi.org/10.1016/0029-554x(62)90155-6).
- [3] H. Blok, J. A. J. M. Disselhorst, S. B. Orlinski, and J. Schmidt, "A continuous-wave and pulsed electron spin resonance spectrometer operating at 275 GHz," *Journal of Magnetic Resonance*, vol. 166, no. 1, pp. 92–99, Jan. 2004, doi: <https://doi.org/10.1016/j.jmr.2003.10.011>.
- [4] H. Yokoyama and T. Yoshimura, "Combining a Magnetic Field Modulation Coil with a Surface-Coil-Type EPR Resonator," *Applied Magnetic Resonance*, vol. 35, no. 1, pp. 127–135, Nov. 2008, doi: <https://doi.org/10.1007/s00723-008-0148-y>.
- [5] G. Mitrikas, Y. Sanakis, C. P. Raptopoulos, G. Kordas, and G. Papavasiliou, "Electron spin-lattice and spin-spin relaxation study of a trisubstituted iron(II) complex and its relevance in quantum computing," *Phys. Chem. Chem. Phys.*, vol. 10, no. 5, pp. 743–748, 2008, doi: <https://doi.org/10.1039/b711056a>.
- [6] A. Sojka et al., "Sample Holders for Sub-Tera Electron Spin Resonance Spectroscopy," in *IEEE Transactions on Instrumentation and Measurement*, vol. 71, pp. 1–12, 2022, Art no. 8002812, doi: <https://doi.org/10.1109/TIM.2022.3164135>.
- [7] A. Savitsky, A. Nalepa, T. Petrenko, M. Plato, Klaus Möbus, and W. Lubitz, "Hydrogen-Bonded Complexes of Neutral Nitroxide Radicals with 2-Propanol Studied by Multifrequency EPR/ENDOR," *Applied Magnetic Resonance*, vol. 53, no. 7–9, pp. 1239–1263, Dec. 2021, doi: <https://doi.org/10.1007/s00723-021-01442-y>.
- [8] A. Savitsky and K. Möbus, "High-field EPR," *Photosynthesis Research*, vol. 102, no. 2–3, pp. 311–333, May 2009, doi: <https://doi.org/10.1007/s11120-009-9432-4>.
- [9] L. Song et al., "Toward increased concentration sensitivity for continuous wave EPR investigations of spin-labeled biological macromolecules at high fields," *Science advances*, vol. 9, no. 38, Sep. 2023, doi: <https://doi.org/10.1126/sciadv.adf7412>.
- [10] V. B. Zhukhovitskiy et al., "Reactions of lithium phthalocyanine with various oxidizing agents," *Bulletin of the Academy of Sciences of the USSR Division of Chemical Science*, vol. 34, no. 12, pp. 188–196, Apr. 2016, doi: <https://doi.org/10.1016/j.jm.2016.02.007>.
- [11] "TEMPO," *American Chemical Society*, <https://www.acs.org/molecule-of-the-week/archive/t/tempo.html> (accessed Feb. 20, 2023).
- [12] J. A. Tewart and A. M. Gokhale, "Nearest neighbor distances in uniform-random poly-dispersed microstructures," *Materials Science and Engineering: A*, vol. 396, no. 1, pp. 22–27, Apr. 2005, doi: <https://doi.org/10.1016/j.msea.2004.12.034>.
- [13] P. Willke et al., "Hyperfine interaction of individual atoms on a surface," *Science*, vol. 362, no. 6412, pp. 336–339, Oct. 2018, doi: <https://doi.org/10.1126/science.1254747>.
- [14] Y. E. Kandrasnikin, "Estimation of Heisenberg exchange interaction in rigid photoexcited chromophore-radical compound by transient EPR," *The Journal of Chemical Physics*, vol. 160, no. 4, Jan. 2024, doi: <https://doi.org/10.1063/5.0188404>.